The Korean Journal of Rheology,
Vol. 7, No. 1, April 1995 pp.19-27

〈연구논문〉

원반 형상의 정밀사출성형에 관한 실험적 연구

윤 경 환

단국대학교 기계공학과
(1995년 1월 10일 접수)

An Experimental Study on Precision Injection Molding of Center-gated Disks

Kyunghwan Yoon

Department of Mechanical Engineering, Dankook University,
San 8, Hannam-Dong, Yongsan-Ku, Seoul 140-714, Korea
(Received January 10, 1995)

요 약

정밀사출성형품을 생산하기 위해서는 성형 조건의 변화가 최종 사출품에 어떠한 영향을 미치는 가에 대한 연구가 필요하다. 본 논문에서는 성형조건을 조직적으로 변화시키며 가장 간단한 원반형상의 사출품에 남는 복굴절의 분포를 측정함으로써 성형조건의 변화가 최종 사출품의 광학적 이방성의 구조에 어떠한 영향을 미치는 가에 촛점을 맞추었다. 광탄성적 성질이 많이 다른 폴리스틸렌과 폴리카보네이트를 재료로 지름이 10.16 cm이고 두께가 2 mm인 금형을 사용하였다. 두께 방향의 복굴절양과 광학 주축각의 분포를 통해 보압 크기가 최종 사출품의 광학적 이방성, 특히 내측의 두 개의 정점값에 미치는 영향을 알 수 있었다. 한편, 서로 다른 두 물질의 광학적, 물리적 성질의 차이점에 기인한 복굴절 분포의 구조적 차이점도 발견할 수 있었다. 이 실험 데이터는 컴퓨터 모사에의한 최종 사출품의 잔류 응력과 광학적 이방성 예측에도 중요한 자료가 되리라 믿는다.

Abstract—It is necessary to study the effect of various process conditions on the final injection-molded parts for producing precision injection-molded products. In the present paper we have focussed on the effect of process conditions on the optical anisotropy remaining in the disk-shaped product by varying the process conditions systematically. Polystyrene and polycarbonate, which have different photoelastic properties, were used to mold the disk of the diameter of 10.16 cm and the thickness of 2 mm. By examining the gapwise distribution of birefringence and extinction angle the effect of holding pressure on the structure of optical anisotropy, especially, on the value of inner two birefringence peaks has been shown clearly. Furthermore, structural difference in birefringence data of two different materials have been found which came from the differences in optical and physical properties. This experimental data could serve as a basis of testing the computer simulation program to predict the residual stresses and optical anisotropy distribution in the final injection-molded products.

Keywords: Injection molding, birefringence, optical disk

1. Introduction

Injection molding is one of the most popular processes in the plastic industry. Recently, birth of new engineering plastics made it possible for the more precise articles to be produced through injection molding process. Precision injection molding is a terminology used to cover manufacturing the products whose tolerence is order of micron or less. It goes without saying that final residual stresses should be reduced to make a product of good quality. Understanding the physics involved in whole injection molding process is even more necessary than before.

Extensive literatures [1-6] can be found to study the physical mechanisms forming the final residual stresses and birefringence in injection-molded products by experiments and numerical simulations. Flow-induced and thermally-induced stresses (or birefringence) were usually studied separately. Especially, for the optical products, such as optical disks and plastic lenses, the final optical structure in injection-molded parts itself became important to study. More detailed survey for each mechanism to induce the final stresses and birefringence will be given in section 3.

In our previous research [7, 8], the effect of various process conditions on the birefringence of injection-molded center-gated polystyrene disks were presented by examining the in-plane and gapwise birefringence. In the course of our previous experimental investigation, we found the need for more systematic study with different material and different processes. So, injection-molded disks were made with polycarbonate as well as polystyrene under the various packing pressure condition. Polycarbonate was chosen because it showed different stress optical behavior from polystyrene. In this paper, the detailed experimental birefringence and extinction angle distribution in gapwise direction for polystyrene and polycarbonate disks will be presented and compared.

2. Photoelasticity and Birefringence

In the linear photoelasticity theory, refractive index difference changes with the difference of principal stresses proportionally when the stress is applied to isotropic materials as follows:

$$n_i - n_j = C(\tau_i - \tau_j)$$

where i, j, k=I, II, III & i≠j≠k≠i

And τ_I, τ_{II}, τ_{III} are the principal stresses, that is, the stresses in the direction of the three principal axes, and n_i is the index experienced by a light wave polarized in the direction of the principal axis i. C is the (relative) stress-optical coefficient. This linear stress-optical relationship has been tested and verified in wide range of conditions for various polymeric materials [9]. The stress-optical coefficient for the polystyrene is known about −4800 Brewsters ($1Br=10^{-12}$ Pa^{-1}) above T_g and 8~10 Br in glassy state. The stress-optical coefficient for the polycarbonate is known about 3500~3700 Br above T_g and 60~70 Br in glassy state. Note that sign of the stress optical coefficients for polystyrene and polycarbonate is different above T_g due to the difference in dielectric property of two materials. The dependency of stress-optical coefficient on temperature and time near glass transition temperature, which is known as photo-viscoelasticity, has been studied in detail recently [10].

The geometry and coordinate system of 10.16 cm diameter center-gated disk are shown in Fig. 1. For the simple-shear case like our center-gated disk where shear stresses are in the 1-2 plane, following the notation in [5] the non-zero components of the index tensor are n_{11}, n_{22}, n_{33} and n_{12}.

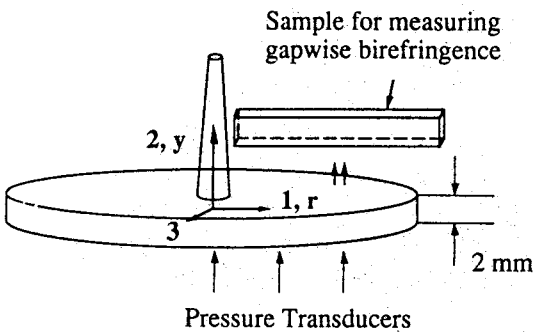

Fig. 1. Sample geometry and the coordinate system in center-gated disk.

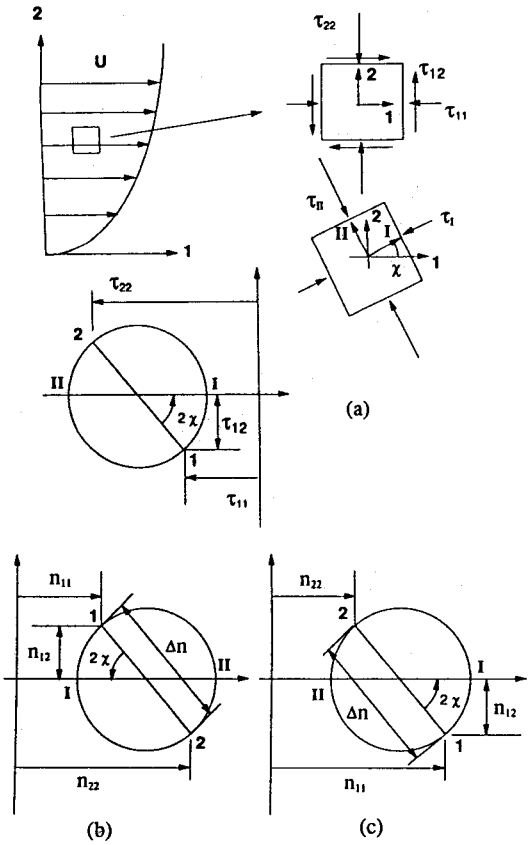

Fig. 2. Stress distribution on the fluid element and its corresponding Mohr's circles of stress for the simple-shear case (a). And Mohr's circle representations for the index of refraction tensor for negative C (b) and positive C (c), respectively.

Figure 2(a) shows the state of stresses imposed on a fluid element under the simple-shear case, which can be described with a Mohr's circle. The angle between the coordinate system and the principal axes is called the extinction angle. By applying the linear stress-optical relation the maximum birefringence Δn in the 1-2 plane and the extinction angle χ can be written as follows;

$$\Delta n \sin 2\chi = 2n_{12} = 2C\ \tau_{12}$$
$$\Delta n \cos 2\chi = n_{11} - n_{22} = 2C(\tau_{11} - \tau_{22})$$
$$|\Delta n| = |C|\sqrt{(\tau_{11} - \tau_{22})^2 + (2\tau_{12})^2}$$

If we keep the sign convention of the stress-optical law carefully, the following expression for Δn is found to be more precise.

$$\Delta n = C\sqrt{(\tau_{11} - \tau_{22})^2 + (2\tau_{12})^2}\ \frac{\tau_{11} - \tau_{22}}{|\tau_{11} - \tau_{22}|}$$

Figure 2(b) and (c) show the state of refractive index tensor in the 1-2 plane as a Mohr's circle. Note that the extinction angle is defined differently for the case of positive and negative stress-optical coefficients. This is necessary to make sure the interpretation of bire fringence and extinction angle data in the section of results for polystyrene and polycarbonate, repectively.

3. Formation of Frozen-in Birefringence

There are four well known phenomena which cause frozen-in birefringence in injection-molded samples.

The fountain flow region in the vicinity of the flow front is believed to form a very thin skin layer with a very high tensile force in the flow direction during the filling stage. However, this layer is difficult to define and discern in the birefringence measurements because cooling effects are also very significant in this region. This fountain flow phenomenon has been reviewed very well in Coyle et al. [11] using flow visualization and numerical techniques. Their illustration shows the deformation history of rectangular elements located at different vertical positions, where the element starting from the middle yields a highly stretched inverse V shape near the wall. Mavridis et al. [12] included the effect of fountain flow in their viscoelastic numerical simulation and showed an extra birefringence peak at the wall in injection-molded plates.

The stress distribution during the filling stage depends on the geometry of the sample. The shear-stress distribution in the gapwise direction is one of the most significant sources for generating high molecular orientation. Isayev and Hieber [13] applied Leonov's viscoelastic model to calculate the stress distribution through the filling and post-filling process with no holding pressure applied. Note that the nondimensional shear rate remains maximum at the wall even though the ac-

tual shear rate becomes negligible due to cooling by the cold wall. The location and the quantative value of predicted gapwise birefringence peak induced from the shear stress and subsequent stress relaxation showed good agreement with Kamal and Tan's [3] experimental data for the polystyrene strip.

After the filling process, the packing (or holding) process affects flow until the gate freezes off. During this process, more material enters the mold to reduce shrinkage of the molded product. Basically, the material whose temperature is still above T_g will still be moving and the orientation formed under the high stress from the post-filling process will remain as two inner birefringence peaks. Note that the stress-relaxation process is dependent on the local temperature and pressure history. Recently, Flaman [14] and Wimberger-Friedl [15] analyzed the whole injection molding process numerically by using a compressible version of Leonov model [16, 17]. The qualitative process for forming two inner birefringence peaks could be explained well. However, the quantitative prediction of birefringence distribution still needs more investigation.

Finally, cooling effect involved throughout the entire injection molding process plays a major role to form a frozen-in birefringence. When hot plastic melt touches the cold mold surface a frozen layer start to grow and penetrate further in from the wall. After flow stops, this cooling and the stress relaxation will be the two dominant processes. Conventional analyses [18-20] for freely quenched plate were very useful to understand the physics involved in forming the residual stresses and birefringence. Recently, researchers [5, 15, 21] paid more attention to the different boundary conditions from free quenching, such as constrained and partially constrained quenching, to emulate the injection molding process more realistically. Their study showed big differences between free and constrained cases for the final structure of residual stresses and birefringence.

To understand and predict the birefringence and stresses in the final molded parts accurate pressure, temperature history and birefringence data are still wanting.

4. Experimental Setup and Sample Preparation

The mold used in [7, 8] was modified to ensure the clamping force to be in the machine's limit. The diameter of the disk was reduced to 10.16 cm and the nominal thickness was 2 mm as shown in Fig. 1. Four Dynisco pressure transducers(465-XL) were flush mounted at the nozzle, under the sprue, 1.905 cm and 3.81 cm apart from the sprue in radial position, respectively. An extra hydraulic pressure on the back side of injection screw was also recorded.

First part of injection-molded samples were made of polystyrene, Dow Styron 615APR via Boy 50T machine and Moog controller. The molding conditions of a melt temperature of 225℃, a mold temperature of 40℃ and injection speed of 23.8 cc/sec were kept constant. The holding (hydraulic) pressure was varied from 0 MPa (no packing) to 4.14 MPa with an increment of 0.69 MPa.

Second part of injection-molded samples were made of polycarbonate, GE Lexan 141-111. The molding conditions of a melt temperature of 300℃, a mold temperature of 80℃ and injection speed of 23.8 cc/sec were kept constant. The holding (hydraulic) pressure was varied as in the same way for polystyrene.

The measurement of birefringence was carried out under the polarizing microscope (Leitz) with a Berek compensator (B and K types). In order to measure the birefringence the samples were cut along the radial direction with a diamond saw and polished with diamond(or aluminum) powder to get the better optical vision. The thickness of cut samples was varied between 0.2 and 0.5 mm. With this method we could get the gapwise profile of Δn (or n_{11}-n_{22}) and extinction angle which will provide more detailed information for understanding the optical structure in the final injection-molded products.

5. Experimental Data and Results

5.1. Injection-molded Polystyrene Disks

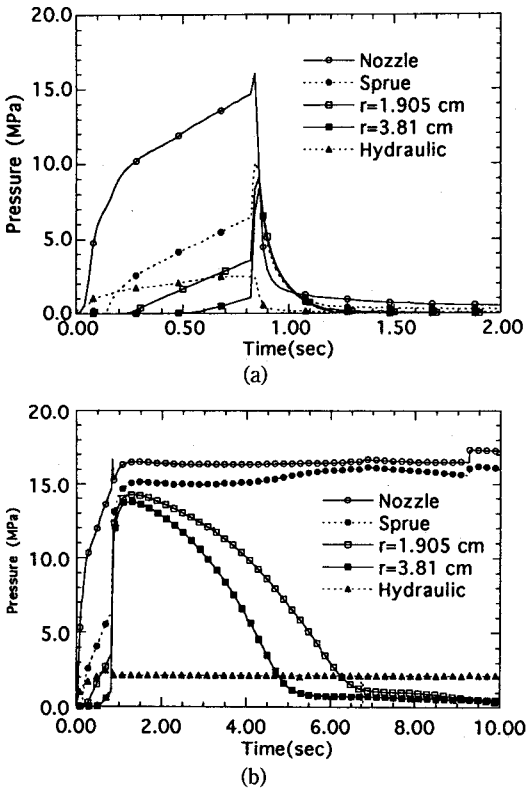

Fig. 3. Pressure traces at various radial locations for packing pressures of 0 MPa (a) and 2.07 MPa.

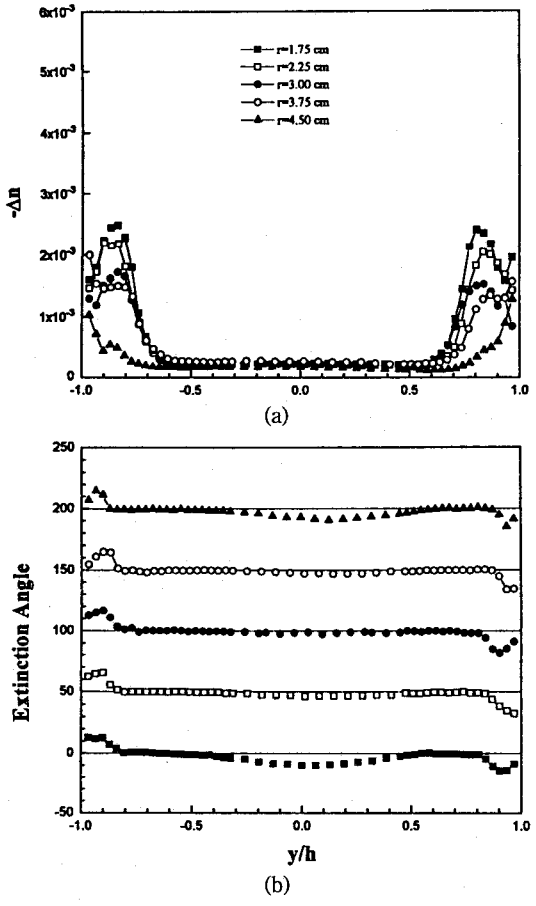

Fig. 4. Gapwise profiles of birefringence Δn (a) and extinction angle (b) of polystyrene disk at various radial locations when no packing pressure applied (The extinction angles for r= 2.25 cm~4.50 cm are shifted by 50 in the plot.).

Figures 3(a) and (b) show the pressure traces at different locations for the case of packing pressure of 0 and 2.07 MPa, respectively. This experimental data is very important to study the process numerically. Predicting the downstream pressure history by using the upstream pressure as an input is very useful practice to conform the models for theory and property data involved in the numerical simulation.

The gapwise distribution of Δn and extinction angle at different radial locations for packing pressures of 0, 2.07 MPa and 3.45 MPa are shown in Figs. 4, 5 and 6, respectively. Henceforth, the horizontal axes in the figures for gapwise distributions are non-dimensionalized based on the half-gap thickness of the disk, h. And positive value of y/h has been kept to the side where the sprue is. Also, note that the birefringence value of Δn for polystyrene is negative following our definition in section 2.

In Figs. 4 (a) and (b), distinct peaks are found at y/h is about ±0.8 for Δn and y/h is about ±0.9 for the extinction angle. These peaks near the mold wall are due to the flow-stress distribution during the filling and subsequent relaxation [13]. The birefringence value of about -2×10^{-4} in the flat inner region in Fig. 4(a) attributed to the thermal stresses developed during the subsequent cooling process after the flow has stopped as explained in section 3.

Fig. 5 shows the effect of packing process on

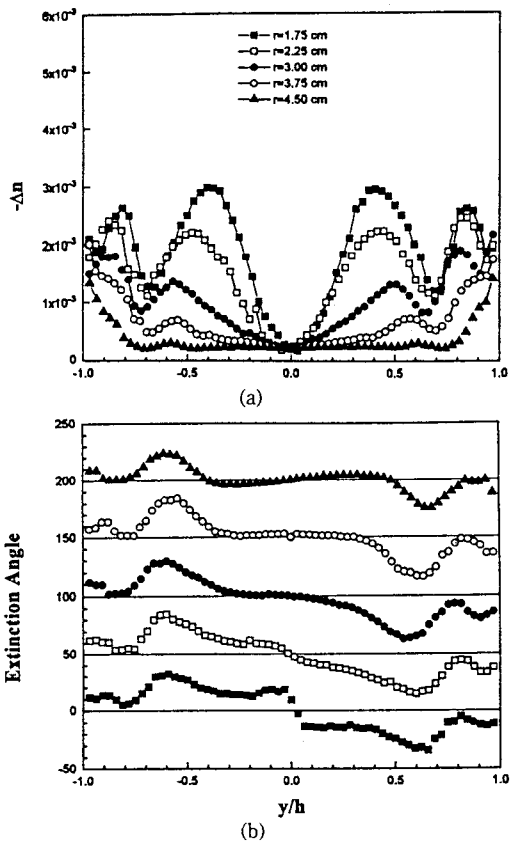

Fig. 5. Gapwise profiles of birefringence Δn (a) and extinction angle (b) of polystyrene disk at various radial locations for hydraulic holding pressure of 2.07 MPa.

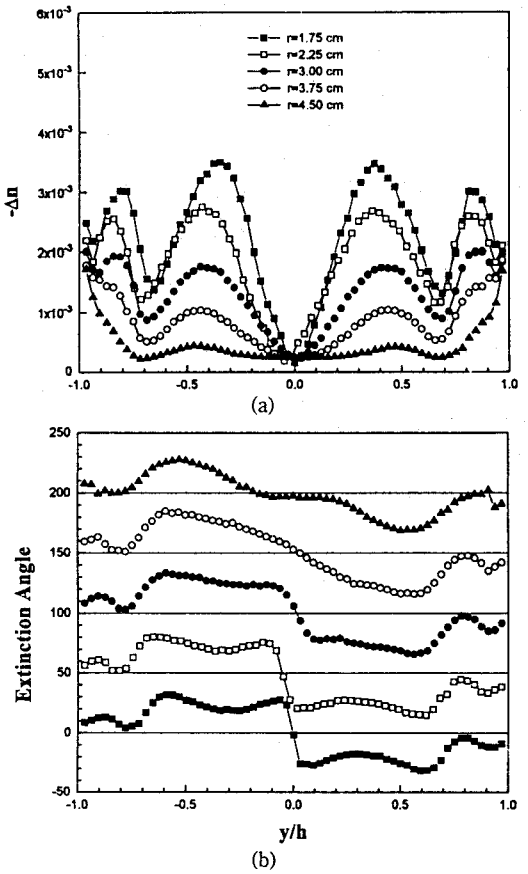

Fig. 6. Gapwise profiles of birefringence Δn (a) and extinction angle (b) of polystyrene disk at various radial locations for hydraulic holding pressure of 3.45 MPa.

the frozen-in birefringence and extinction angle at all radial locations. The general shape of distribution of the birefringence in 1-2 plane, Δn, shows two distinct peaks as shown in Fig. 5(a). The peak near the mold wall ($y/h = \pm 0.8$) is generated from the flow-stress distribution during the filling stage as in the case of no packing. However, the other inner peak is due to the flow during the post-filling stage [14, 15]. Both inner and outer peak values decrease away from the sprue in radial direction. In Fig. 5(b) inner peak can also be found for the extinction angle at y/h is about ± 0.6. At the center ($y/h = 0$), where the theoretical extinction angle should be exactly zero, the birefringence value still shows about -2×10^{-4} as no packing case.

Fig. 6 shows the effect of higher packing for both the birefringence and extinction angle. Near the sprue the extinction angle shows the hump rather than a single peak pattern for the inner birefringence peak zone. Near the central zone less flow-induced and more thermally-induced birefringence results in this pattern.

5.2. Injection-molded Polycarbonate Disks

The gapwise distribution of Dn and extinction angle at different radial locations for packing pressures of 0, 2.07 MPa and 3.45 MPa are shown in Figs. 7, 8 and 9, respectively. Note that the birefringence for polycarbonate always shows positive value following our definition.

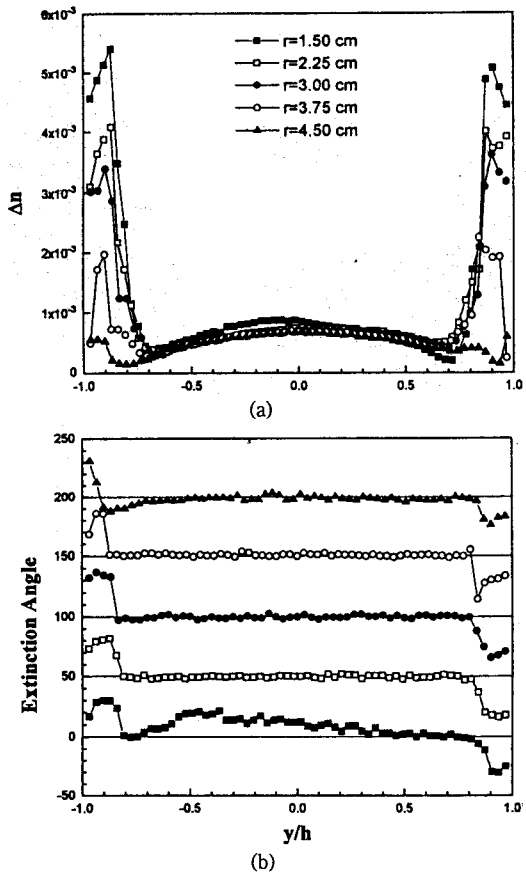

Fig. 7. Gapwise profiles of birefringence Δn (a) and extinction angle (b) of polycarbonate disk at various radial locations when no packing pressure applied.

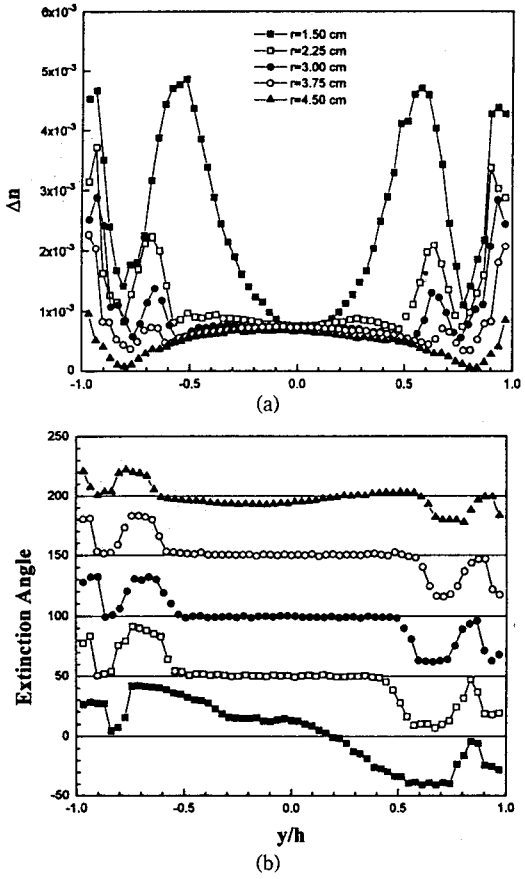

Fig. 8. Gapwise profiles of birefringence Δn (a) and extinction angle (b) of polycarbonate disk at various radial locations for hydraulic holding pressure of 2.07 MPa.

In Figs. 7 (a) and (b), no inner peak (induced by post-filling process) was found as with polystyrene. However, the birefringence shows about 8×10^{-4} at the center and decreases as well-known papabolic pattern [19, 20]. This pattern of birefringence would emulate the residual thermal stress pattern for the constrained quenching [5, 15, 21] rather than the case of free quenching. From the results for the extinction angle in Fig. 7 (b), which is almost zero in the region of $-0.7\leq y/h\leq 0.7$, we can conclude that this parabolic birefringence pattern is mostly due to the thermally-induced stresses.

Fig. 8 shows the case of packing pressure of 2.07 MPa. The general shape of distribution of the birefringence is similar to the case of polystyrene. However, except the radial location near the sprue, less flow-induced and more thermally-induced effect have been found for polycarbonate than for polystyrene.

Fig. 9 shows the case of packing pressure of 3.45 MPa. At the most radial locations the effect of higher packing can be found for the inner peak value of birefringence as in the case of polystyrene. However, the inner peak value was found to be less for higher packing case at the radial location of 1.50 cm apart from the sprue. Probably it is due to the rapid relaxation process during the post-filling stage. Numerical simulation including proper viscoelastic property data could exp-

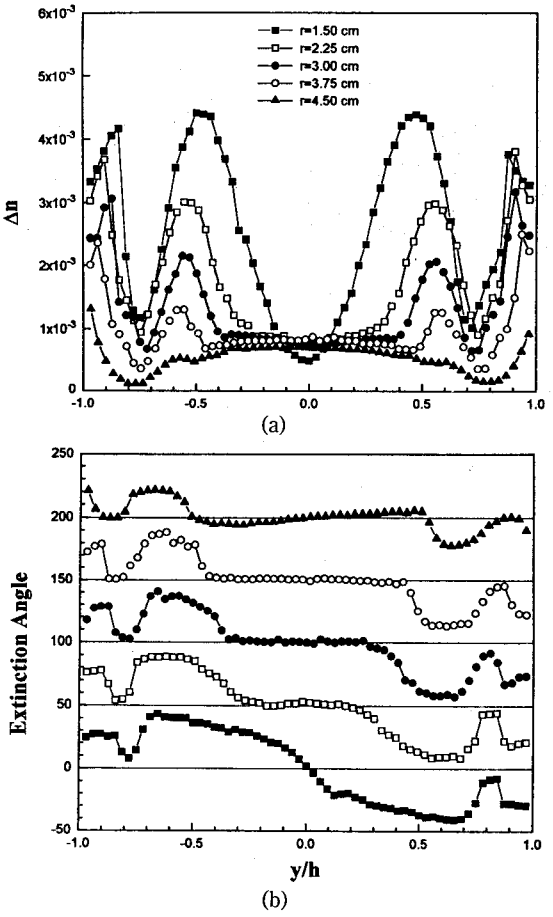

Fig. 9. Gapwise profiles of birefringence Δn (a) and extinction angle (b) of polycarbonate disk at various radial locations for hydraulic holding pressure of 3.45 MPa.

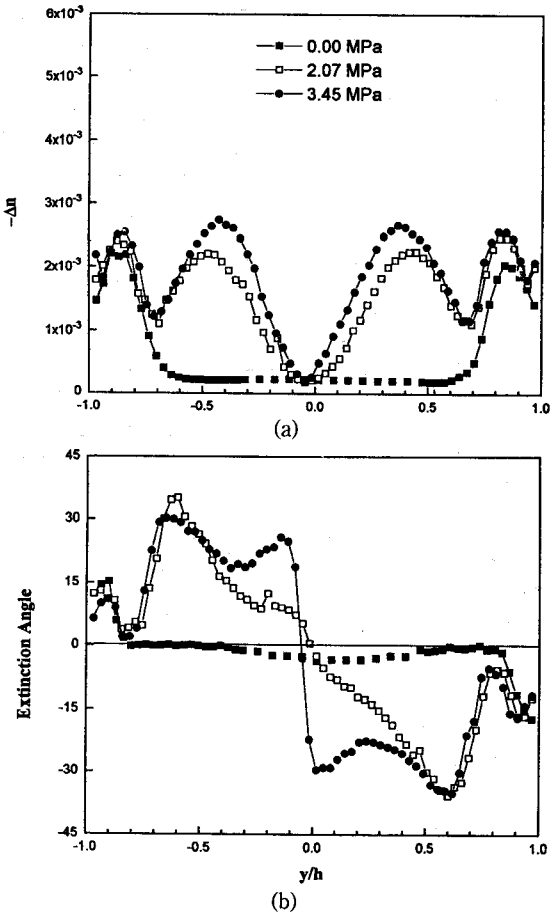

Fig. 10. Gapwise profiles of birefringence Δn (a) and extinction angle (b) of polystyrene disk at r=2.25 cm for hydraulic holding pressures of 0, 2.07 and 3.45 MPa.

lain this kind of experimental results.

6. Conclusions

The effect of the packing pressure on the final birefringence and extinction angle for injection-molded polystyrene and polycarbonate disks has been examined experimentally.

Fig. 10 summarized the typical pattern of the final birefringence structure for all three polystyrene cases at r=2.25 cm. Outer peak values are almost same for both birefringence and extinction angle regardless of packing level. However, inner peak pattern for the extinction angle changes to hump by increasing the packing pressure level.

Fig. 11 shows the final birefringence structure at r=2.25 cm for all polycarbonate cases including two extra cases. Those two cases were not shown in the previous section because of the limitation of space. For the outer peak values of both birefringence and extinction angle the same explanation as in the case of polystyrene is effective. By increasing the packing pressure more effect on the peak value of birefringence can be found clearly in the middle as shown in Fig. 11(a). It is clearly due to the fact that extra molten plastics is injected in the cavity during the post-filling stage. For the extinction angle in the inner birefringence

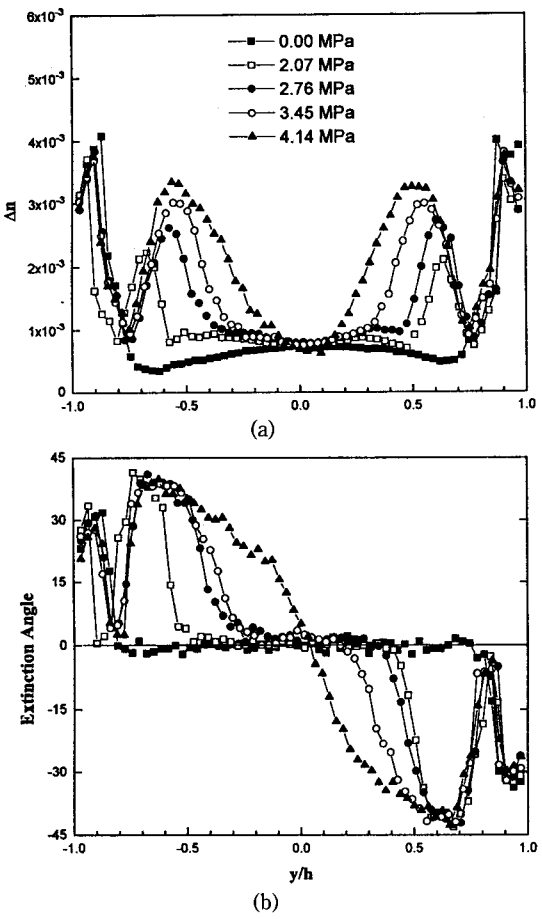

Fig. 11. Gapwise profiles of birefringence Δn (a) and extinction angle (b) of polycarbonate disk at r=2.25 cm for hydraulic holding pressures of 0, 2.07, 2.76, 3.45 and 4.14 MPa.

peak zone a typical single peak pattern rather than a hump pattern was found with polycarbonate.

The experimental data for the materials with different optical and physical properties should serve as a basis of understanding and predicting the residual stresses and optical anisotropy distribution in the precision injection-molded products.

Acknowledgements

This work is supported by Korea Ministry of Education through Mechanical Engineering Research Fund (ME93-E-19), for which the author is grateful. The author also would like to thank Dr. C. A. Hieber and Professor K.K. Wang at Cornell university for their suggestions and discussion in the course of this study.

References

1. G. Menges and G. Wibken, S.P.E. Tech. Papers, **19**, 519-522 (1973).
2. W. Dietz, J.L. White and E.S. Clark, *Polymer Eng. & Sci.*, **18**(4), 273-281 (1978).
3. M.R. Kamal and V. Tan, S.P.E. Tech. Papers, **24**, 121-126 (1978).
4. J. Greener and G.H. Pearson, *J. Rheology*, **27**, 115-134 (1983).
5. A.I. Isayev, "Injection and Compression Molding Fundamentals", Marcel Dekker Inc., New York and Basel, 1987.
6. B.L. Evans, *J. Mat. Sci.*, **24**, 3588-3598 (1989).
7. K. Yoon and K.K. Wang, S.P.E. Tech. Papers, **37**, 333-337 (1991).
8. K. Yoon and K.K. Wang, S.P.E. Tech. Papers, **38**, 2221-2225 (1992).
9. H. Janeschitz-Kriegl, "Polymer Melt Rheology and Flow Birefringence", Springer-Verlag, Berlin, 1983.
10. G.D. Shyu, Ph.D. Thesis, The Univ. of Akron (1993).
11. D.J. Coyle, J.W. Blake and C.W. Macosko, *AIChE Journal*, **33**, 1168-1177 (1987).
12. H. Mavridis, A.N. Hrymak and J. Vlachopoulos, *J. Rheol.*, **32**, 639-663 (1988).
13. A.I. Isayev and C.A. Hieber, *Rheol. Acta*, **19**, 168-182 (1980).
14. A.A.M. Flaman, Ph.D. Thesis, Eindhoven Univ. of Tech (1990).
15. R. Wimberger-Friedl, Ph.D. Thesis, Eindhoven Univ. of Tech (1991).
16. A.I. Leonov, *Rheol. Acta*, **15**, 85 (1976).
17. A.I. Leonov, E. Kh. Lipkina, E.D. Paskhin and A. N., Prokunin, *Rheol. Acta*, **15**, 411 (1977).
18. B.D. Aggarwala and E. Saibel, *Phys. Chem. Glasses*, **2**, 137-140 (1961).
19. E.M. Lee, T.G. Rogers and T.C. Woo, *J. Amer. Ceram. Soc.*, **48**, 480 (1965).
20. C.J. Wust and D.C. Bogue, *J. Appl. Polym. Sci.*, **28**, 1931-1947 (1983).
21. N. Santhanam, Ph.D. Thesis, Cornell University (1992).